COMBINED SIMULATION METHOD FOR IMPROVED PERFORMANCE IN GRID INTEGRATION STUDIES INCLUDING MULTI-TERMINAL VSC-HVDC

Arjen A. van der Meer*, Ralph L. Hendriks, Madeleine Gibescu
Jan A. Ferreira, Mart A. M. M. van der Meijden, Wil L. Kling

* Delft University of Technology, the Netherlands, e-mail: A.A.vanderMeer@tudelft.nl

Keywords: combined simulations, VSC-HVdc, transient stability, time-domain simulations

Abstract

This paper presents an interfacing method to combine stability-type simulations with electro-magnetic transients (EMT) calculation. The stability-type simulation is coupled with the EMT simulation by Thévenin-equivalent variable source representations, whereas the EMT-type simulator is connected to the stability-type simulation by Fourier analysis. The paper describes this procedure and elaborates on the numerical performance of this mutual coupling, which is done by studying an exemplary test case. The focus is on integrating multi-terminal VSC-HVdc schemes in stability-type simulations.

1 Introduction

In view of possible future offshore network developments, an important topic of study is the impact of multi-terminal high-voltage dc transmission based on voltage sourced converter technology (VSC-HVdc) on the transient stability of the power system. Stability issues in ac systems are usually investigated using simulation tools that are based on a well-defined framework of assumptions. As the focus is on electro-mechanical interactions, the network can be represented by quasi steady-state phasors and can be assumed balanced. The phenomena of interest occur in a frequency range from about 0.1 to 10 Hz, requiring simulation times of several seconds or longer. Due to aforementioned simplifications simulation time-step sizes up to half a cycle can be realised, keeping computation times reasonable.

The incorporation of VSC-HVdc transmission into stability-type simulations is a challenge. The dynamics of power electronic converters and dc networks are generally fast (microseconds range), exceeding the bandwidth normally applied in transient stability studies. This dynamic behaviour is, therefore, in itself not relevant to be considered in transient system stability studies, notwithstanding that these fast dynamics might result in activation of control and protection functions (e.g. converter blocking, power ramping) that could result in important low-frequency interactions with the ac power system. In models of point-to-point VSC-HVdc transmission this behaviour is usually successfully incorporated by heuristic rules. For the accurate simulation of multi-terminal VSC-HVdc links a better structured modelling and simulation method is required. Ideally, such methods will not compromise the excellent computational performance of transient stability simulators. Conventionally, power electronic converters and dc networks can be studied in detail by simulation of electro-magnetic transients (EMT). In EMT simulators the electric network is represented by differential equations and as a result the required integration time-step size is much smaller than for stability simulators. Also, as the underlying models are much more elaborate, the data requirements are higher. EMT simulations have been successfully applied on component level and for controller design, but are generally not suitable for the simulation of larger systems due to prohibitively long computation times.

This paper introduces the basic principles of combining stability-type and EMT-type numerical simulators. By modelling only selected parts of the system in the EMT simulation and the remainder in the stability simulation, both accuracy and computational speed requirements for the simulation of large systems can be met with a single procedure. The combined simulation method potentially has a wide area of application within power engineering as it provides a high level of flexibility regarding the connection of different types of models and simulation methods to each other. This paper elaborates on the numerical implementation of combining the two types of simulators and on the inclusion of multi-terminal VSC-HVdc networks into this framework. Simulations have been performed with a modelling framework developed in Matlab and are validated against a full EMT-type simulation executed in PSS®NETOMAC.

The paper is organised as follows. First, the combined simulation method will be presented by introducing the interfacing techniques necessary for achieving a correct coupling between both types of simulation. The paper continues with the implementation of VSC-HVdc schemes within the proposed method. A small test network has been designed to exhibit the differences between several implementations of the interface. The paper ends with conclusions and recommendations for further work.

2 Combined simulation method

Combined time-domain simulations for power systems were first proposed in the 1980s and have been improved in the

folowing decades [3, 7, 9]. These contributions focused mainly on classical HVdc. Currently, the *IEEE task force on interfacing techniques for simulation tools* elaborates on the coupling of several power system simulation tools, including EMT-type and stability-type simulators [5].

Traditionally, stability-type simulators assume a fundamental-frequency, balanced set of three-phase voltages and currents, which allows representing the network as a positive-sequence single-line equivalent. Moreover, electro-magnetic interactions between network elements are considered insignificant to the system-wide electro-mechanical oscillations exhibited by rotating machinery. Therefore, network quantities are represented by quasi-stationary complex phasors appearing as algebraic variables in the solution scheme of the simulation. EMT-type simulations include network elements by differential equations, and corresponding network quantities are represented by waveforms. This allows simulation to a greater level of detail, at the cost of a much smaller time-step size.

To couple these different types of simulation, information about network quantities must be interfaced accurately. Hence, the coupling scheme consists of

- a proper network setup around the coupling location;
- a robust transformation of variables (currents, voltages) between both simulations; and
- an interaction protocol that describes the interface order in time.

The coupling location can be a single node or a network segment. The network simulated in EMT is denoted by the detailed network whereas the network simulated by the stability-type simulation is defined as the external network. The stability-type and EMT-type simulators are executed sequentially in time. The stability-type simulation uses a fixed time-step size h whereas the EMT-type simulation employs a time-step size h_{emt}, which is chosen much smaller. The EMT-type simulator is hence included into the solution scheme of the stability-type simulator.

2.1 Network setup

Around the coupling location, the network must be included in both types of simulation. In this paper, the coupling location is a single node, the interface node. Key to the accuracy of the combined simulation method is the way in which the external system in the stability-type simulation is represented in the detailed network, which includes the VSC network interface and the dc network. This is due to the fact that the EMT-type simulation is included into the stability-type simulation as a minor integration loop which is executed each calculation step of the stability-type simulator. Hence, network quantities can be updated only once per calculation step of the stability-type simulation. This issue can be resolved by employing frequency-dependent equivalent representations of network quantities and branches, such as the branch companion approach [8] and the

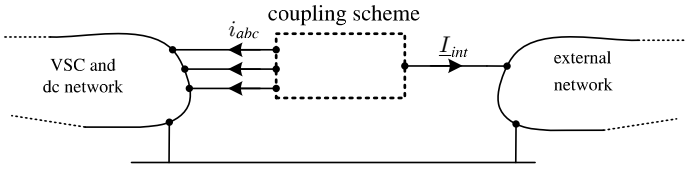

Figure 1: Generalised representation of the coupling between the external network and the network in EMT

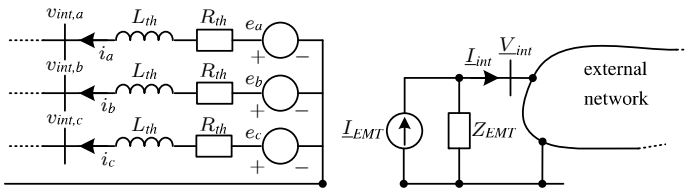

Figure 2: Applied network setup around interface location

adaptation of coherency-based wide-band equivalents [6]. A generalised scheme is shown in Fig. 1.

Here, the external network is represented by a Thévenin-equivalent impedance in series with a variable voltage source. This impedance, denoted by $Z_{th} = R_{th} + \mathrm{j}\omega L_{th}$, is calculated during the initialisation procedure and remains unaltered during the time-domain simulation. Despite the fact that the actual Thévenin impedance will vary, particularly during faults, it is considered sufficient to compensate this by updating the Thévenin voltage-source only, as adjusting the Thévenin impedance requires numerically complex re-initialisation of currents and voltages each time the equivalent is updated [1]. In the same fashion, the detailed system is represented into the external system by a fundamental frequency Norton-equivalent whose variable current injection is updated after every calculation run of the EMT-type solver. The adapted network setup at the interface location is summarised in Fig. 2.

2.2 Interaction procedure

Conventionally, the set of differential-algebraic equations inherent to stability-type simulations are solved using a predictor-corrector method [4]. At the end of the previous stability-type simulation calculation step, denoted by t_n, all network quantities are known and disturbances can be applied. Subsequently, machine and network quantities are predicted according to the discretized differential equations, comprising the predictor part of the solution scheme. The corrector part uses the resulting quantities to iteratively find the correct network solution at $t_{n+1} = t_n + h$. The Norton current injection at the interface node is considered not to change within this time frame, which allows updating this source at $t = t_n$ only.

This paper considers two interaction procedures, i.e. ways in which the EMT-solver in incorporated into the solution scheme; both are depicted in Fig. 3. In the interaction procedure of Fig. 3a, the stability-type solver uses solely information about previous calculation steps, whereas Fig. 3b shows an alternative order in which network quantities are exchanged.

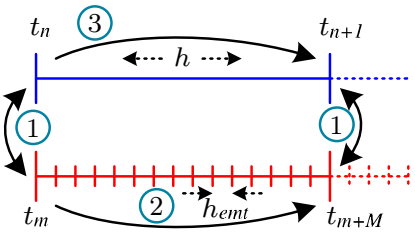

(a) Conventional interaction protocol

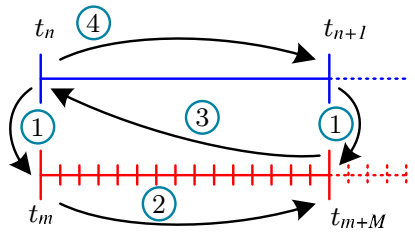

(b) Alternative solution scheme

Figure 3: Numerical interface between stability-type and EMT-type simulation

This order first calculates the inner EMT loop (from t_{m+1} to t_{m+M}, with $M = h/\,h_{EMT}$) before executing the predictor step. It bears the benefit of using information about the detailed parts before assessing the external network. This may improve accuracy, particularly in the case that the influence of power electronic devices on power system dynamics are to be examined. More sophisticated interaction procedures, such as for parallel-wise calculation methods, are summarised in [5].

2.3 Transformation of network quantities

Calculating network values and implementing the interaction procedure requires a suitable transformation of network quantities from one simulation environment to the other. At $t_n = t_m$, the Thévenin equivalent voltage of the stability-type simulation can be determined by

$$\underline{E}_{th} = \underline{V}_{int} + \underline{I}_{int} Z_{th} = E_{th} e^{\mathrm{j}\theta_{th}} \tag{1}$$

in which $\underline{V}_{int}$ is the interface node voltage phasor, $\underline{I}_{int}$ is the phasor of the current flowing into the external system, Z_{th} is the Thévenin-equivalent impedance, and $\underline{E}_{th} = E_{th}\mathrm{e}^{\mathrm{j}\theta_{th}}$ is the dynamic Thévenin equivalent source. Subsequently, the network quantities of the balanced three-phase source in the EMT-part of the system are updated according to

$$\begin{aligned} e_a^{t_m} &= \frac{\sqrt{2}}{\sqrt{3}} E_{th}^{t_n} \cos\left(\delta_{ref}^{t_m} + \theta_{th}\right) \\ e_b^{t_m} &= \frac{\sqrt{2}}{\sqrt{3}} E_{th}^{t_n} \cos\left(\delta_{ref}^{t_m} + \theta_{th} - \frac{2\pi}{3}\right) \\ e_c^{t_m} &= \frac{\sqrt{2}}{\sqrt{3}} E_{th}^{t_n} \cos\left(\delta_{ref}^{t_m} + \theta_{th} + \frac{2\pi}{3}\right) \end{aligned} \tag{2}$$

with

$$\delta_{ref}^{t_m} = \int_0^{t_m} \omega_{ref}^{t_n}\,\mathrm{d}t + \delta_0 \tag{3}$$

and $\omega_{ref}^{t_n}$ the frequency of the slack generator or reference node in rad s^{-1} at time t_n. Amplitude, frequency, and phase angle are kept fixed until the next update instance, at $t_{n+1} = t_n + h$. The variable Norton equivalent source is to be updated at $t = t_n$ or $t = t_{n+1}$, dependent on the applied interaction procedure. The Norton equivalent impedance is included in the network admittance matrix of the stability type-simulation. For the Norton current injection it holds that

$$\begin{aligned} \underline{I}_{EMT} &= \frac{\underline{E}_{th,EMT}}{Z_{EMT}} \\ &= \frac{\underline{V}_{int,EMT} - \underline{I}_{int,EMT} Z_{EMT}}{Z_{EMT}} \end{aligned} \tag{4}$$

where $\underline{V}_{int,EMT}$ and $\underline{I}_{int,EMT}$ are the interface node voltage and current phasors in the EMT-type solver. These phasors have to be calculated from the three-phase waveforms, which can be done by any suitable Fourier technique. As balanced conditions are assumed, the current phasor is computed as the positive sequence component of the interface currents. If undistorted, these currents are described by single sinusoidal components as

$$\begin{aligned} i_r &= \hat{i}\cos\left(\omega_{ref}\, t_m + \phi_r\right) = \hat{i}\cos\left(\frac{2\pi}{N} m + \phi_r\right) \\ &= \frac{\hat{i}}{2}\left[e^{\mathrm{j}\left(\frac{2\pi}{N} m + \phi_r\right)} + e^{-\mathrm{j}\left(\frac{2\pi}{N} m + \phi_r\right)}\right] \end{aligned} \tag{5}$$

with $r = \{a, b, c\}$, $\hat{i}$ the current amplitude, m the EMT calculation step, ϕ_r the phase angle with respect to the EMT reference source, and N the amount of EMT simulation steps that span one fundamental period, i.e. $N = \frac{\omega_{ref}\, h_{emt}}{2\pi}$. The spectral coefficients of the discrete Fourier transform are

$$\begin{aligned} a_{k,r} &= \frac{1}{N} \sum_{p=m-N}^{m} i_r(t_p) e^{\mathrm{j}\frac{2\pi}{N} k m} \\ &= A_{k,r} e^{\mathrm{j}\theta_{k,r}} \end{aligned} \tag{6}$$

with k the k^{th} harmonic component. Only the fundamental frequencies are of interest in this case, i.e. $k = \{-1, 1\}$ and as the current is real, $a_k = a_{-k}^*$. By the time-shifting property, the current phasors can be derived from the spectral coefficients by

$$\underline{I}_r = I_r e^{\mathrm{j}\phi_r} = \sqrt{2} A_{k,r} e^{\mathrm{j}\theta_{k,r}} e^{-\mathrm{j}\delta_{ref}^{t_{m-N}}} \tag{7}$$

The positive-sequence component of the current can now be obtained by

$$\underline{I}_{int,EMT} = \frac{1}{3}\left(\underline{I}_a + \underline{I}_b e^{\mathrm{j}\frac{2\pi}{3}} + \underline{I}_c e^{-\mathrm{j}\frac{2\pi}{3}}\right) \tag{8}$$

A similar approach can be applied for determination of $\underline{V}_{int,EMT}$.

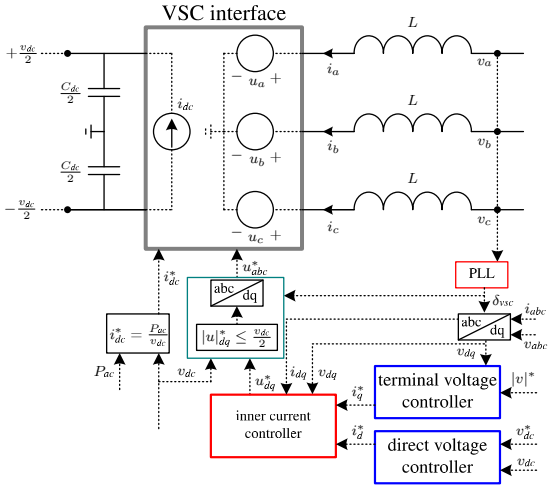

Figure 4: Averaged VSC model using vector control

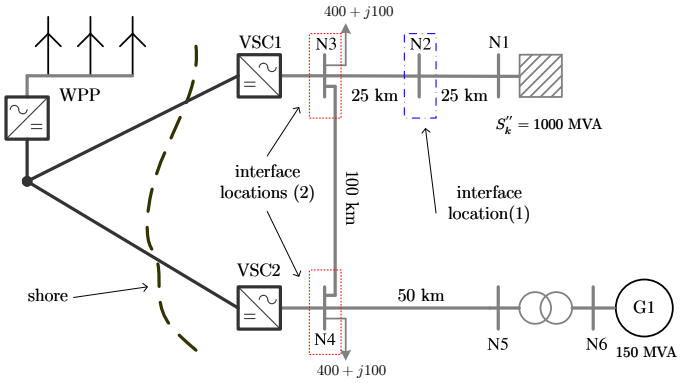

Figure 5: Network used for testing the combined simulation method.

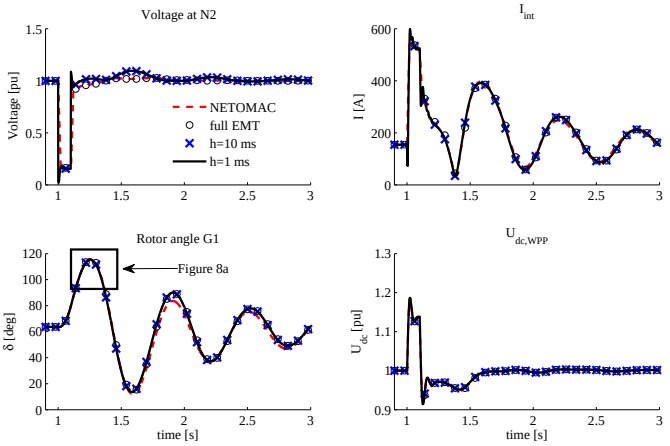

Figure 6: System response with N2 picked as interface location (case 1)

2.4 Implementation of VSC-HVdc

In this paper, VSCs will be modelled in the EMT-type simulation according to the averaged model, which implementation is schematically shown in Fig. 4. Vector control is used to regulate active and reactive power [2], letting the VSC operate as a voltage controlled current source. The control scheme consists of a synchronisation loop and a cascaded control scheme, which contains relatively slow outer controllers and inner current controllers with much shorter settling times. As VSCs have almost no over-current capability, current limits are enforced by the control scheme, giving priority to the part of the current that controls the active power. In case the interface node is at the VSC point of common coupling (PCC), the phase reactor of the VSC equals the Thévenin equivalent impedance, which simplifies the setup of the ac section in the EMT-type simulation.

3 Case studies

The proposed combined simulation method is tested on the network shown in Fig. 5. It consists of two 300 MVA rated VSC terminals connected to a small ac network, which contains a slack node with a short-circuit power of 1000 MVA, and a relatively small generator such that differences between several implementations of the coupling scheme are exhibited. The dc link consists of a 500 MW-rated offshore WPP, modelled by a variable power source, and employing appropriate power reduction mechanisms in case of onshore faults. Simulations have been executed in a Matlab simulation framework, that includes a stability-type simulation as well as an EMT-type simulator [10]. The simulations have been verified against a full EMT simulation executed in PSS®NETOMAC.

3.1 Case 1

In the first case study, the coupling location is set at N2 (see Fig. 5). This implies that the largest part of the network is simulated by the EMT-type solver whereas the small section containing the infinite bus is included into the stability-type simulation. Although this case might be unrealistic in practice, it shows how the EMT part of the simulation interacts with the stability in case the latter is small. This interaction is shown by creating a 100 % balanced voltage dip at the infinite bus, which is cleared after 100 ms. Two different time-step sizes ($h = 1$ ms and $h = 10$ ms) for the stability-type simulation have been chosen, employing the interaction procedured shown in Fig. 3b. The network responses are compared in Fig. 6.

It can be noticed that both EMT-type solutions lie very close to each other. The differences with respect to the reference simulation can to a large extent be attributed to numerical issues, such as a slightly different network solution method and a synchronous generator model that is coupled to the network by a current source instead of a voltage source. These deviations accumulate during the course of the post-disturbance period, which can most prominently be observed when considering the rotor angle response of G1. The combined simulation largely matches the EMT-type simulation. The most substantial differences can be observed at the interface voltage amplitude, which can be explained by the fact that the electro-magnetic interactions between N2 and the infinite grid are now not taken

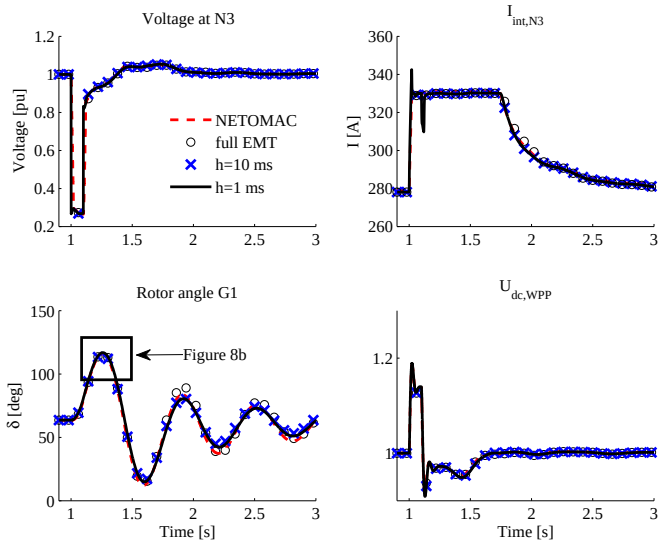

Figure 7: System response with N3 and N4 picked as interface locations (case 2)

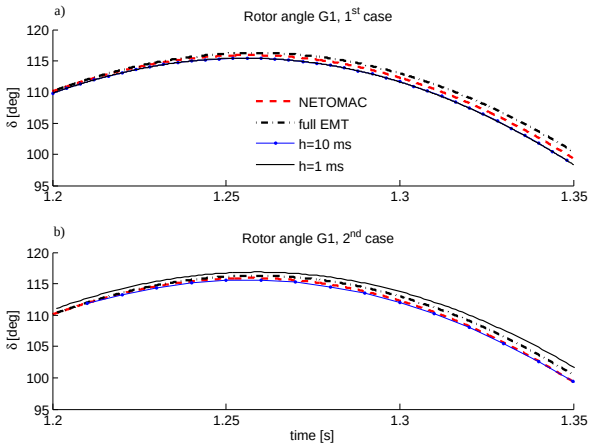

Figure 8: Highlight of rotor angle responses of two different interface locations.

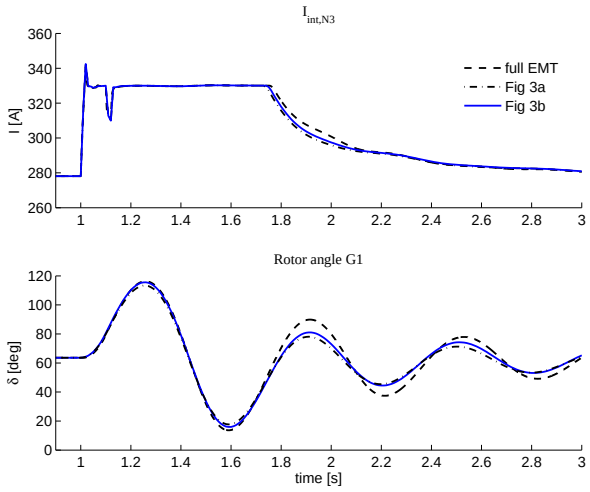

Figure 9: Influence of the interaction protocol on simulation accuracy.

into consideration any longer. According to the rotor angle response, which is highlighted in Fig. 8a, the effect of this difference on the accuracy of the EMT-type simulation remains very small. Furthermore, the time-step size of the stability-type simulation has no influence as the part of the network simulated in this solver contains only algebraic relations.

3.2 Case 2

In practice, it is more convenient to model only those parts in EMT that require more detailed attention, such as converters and the dc network. Therefore, the coupling locations are set to N3 and N4, the PCCs of each VSC. The post-disturbance network response around N3 is shown in Fig. 7. Contrary to the previous case, the interface voltage amplitude shows better resemblance with the EMT-type simulation. This can be attributed to the larger size of the external system, which now contains G1 too, providing a more accurate dynamic response. The peaks in I_{int} after the fault can be explained by the resynchronisation response of the VSC after fault inception and clearance. The direct voltage of the WPP as well as the generator response (Fig. 8b) show good numerical performance, which entails an accurate coupling between both parts of the simulation. In order to show the difference in simulation accuracy between the two proposed interaction procedures, the second case has been repeated with the interaction procedure defined by Fig. 3a, yielding the simulation results shown in Fig. 9. Network quantities are updated with a delay of h, which gives slightly less accurate results. This gives preference for the utilisation of the interaction protocol of Fig. 3b.

3.3 Execution times

A reasonable argument for applying combined simulations is that these have a notable improvement in execution times compared to full EMT. Table 1 shows the measured execution times of the cases shown in Fig. 6 and Fig. 7. For the test network introduced in this paper, the combined simulation is faster. The differences with respect to the full EMT-type simulation are larger in case the interface node is chosen directly at the PCCs. This can be explained by the fact that the network simulated by EMT is considerably smaller compared to case 1, where only the network around the slack node was included in the stability-type simulation.

The test set-up developed in Matlab is approximately three times slower than simulating the same network in PSS®NETOMAC. This can be attributed to the fact that the latter uses well-optimised network solution methods. Rather than optimising execution times for one particular method, the simulation environment in Matlab was developed to test the solution schemes themselves and their mutual integration. Hence, it is more sensible to compare the combined simulation execution times to the full EMT-type simulation performed with Matlab.

	case 1	*case 2*
full EMT	31.90	31.90
Combined $h = 10\,\text{ms}$	27.21	14.16
Combined $h = 1\,\text{ms}$	31.44	18.24

Table 1: Measured execution time per second simulation time

4 Conclusions

At the transmission level, power electronic converter technology is becoming mature. In Western-Europe the grid (inter)connection of offshore wind power through VSC-HVdc is under consideration. As these dc infrastructures will become an integral part of the power system, it is key to examine the interaction between these schemes and the existing ac system, which could have impact on stability. Current time-domain simulation tools do not offer adequate methods to include multi-terminal VSC-HVdc networks into large-scale ac network models.

This paper addressed this issue by introducing a procedure that combines stability-type simulations and EMT-type simulations. This was achieved by modelling VSC terminals and the dc part of the system in an EMT-type simulator while including the remainder of the system in a stability-type simulation. The paper discussed several issues that arise when coupling these simulations and a generally applicable, robust interfacing procedure was shown to have good numerical performance.
It turned out that the numerical accuracy is slightly better in case the interface location is chosen at the PCCs of the VSC terminals, though it must be noted that this holds for the applied test network and hence no conclusions with respect to generalised network structures can be drawn based on this observation. Execution times of the performed studies were measured and it can be concluded that considerable speed gain is achieved when only selective parts of the network are simulated in full detail. In case the additional Fourier calculations and exchange operations take less computation effort than simulating the device and its surrounding network in EMT, then the combined simulation is competitive. In this paper, that was the case and hence a 40 % to 55 % speed improvement was achieved. For large networks, in which a larger part can be simulated in the stability part, this speed gain is expected to further increase.

Future work will focus on generalisations with respect to the network setup around the interface location and the performance of the proposed combined simulation method during unbalanced conditions, inrush currents, and harmonic distortions. Furthermore, the gain in execution times measured in Matlab are expected to be reflected into commercial packages as well. Future work will discuss the correctness of this assumption.

5 Acknowledgements

This research is financially supported by Agentschap NL, an agency of the Dutch Ministry of Economic Affairs, under the project North Sea Transnational Grid (NSTG). NSTG is a joint project of Delft University of Technology and the Energy Research Centre of the Netherlands.

References

[1] J. Arrillaga and N. R. Watson. *Computer Modelling of Electrical Power Systems*. John Wiley, Chichester, UK, 2 edition, 2002.

[2] V. Blasko and V. Kaura. A new mathematical model and control of a three-phase AC-DC voltage source converter. *IEEE Transactions on Power Electronics*, 12(1):116–123, 1997.

[3] M.D. Heffernan, K.S. Turner, J. Arrillaga, and C.P. Arnold. Computation of a.c.-d.c. system disturbances - parts I, II, and III. interactive coordination of generator and convertor transient models. *IEEE Transactions on Power Apparatus and Systems*, PAS-100(11):4341–4363, 1981.

[4] W. D. Humpage and B. Stott. Predictor-corrector methods of numerical integration in digital-computer analyses of power-system transient stability. *Proceedings of the Institution of Electrical Engineers*, 112(8):1557–1565, 1965.

[5] V. Jalili-Marandi, V. Dinavahi, K. Strunz, J. A. Martinez, and A. Ramirez. Interfacing techniques for transient stability and electromagnetic transient programs IEEE task force on interfacing techniques for simulation tools. *IEEE Transactions on Power Delivery*, 24(4):2385–2395, 2009.

[6] Y. Liang, X. Lin, A. M. Gole, and M. Yu. Improved coherency-based wide-band equivalents for real-time digital simulators. *Power Systems, IEEE Transactions on*, PP(99), 2010.

[7] J. Reeve and R. Adapa. A new approach to dynamic analysis of ac networks incorporating detailed modeling of dc systems - parts I and II. *IEEE Transactions on Power Delivery*, 3(4):2005–2019, 1988.

[8] K. Shintaku and K. Strunz. Branch companion modeling for diverse simulation of electromagnetic and electromechanical transients. *Electric Power Systems Research*, 77(11):1501–1505, 2007.

[9] M. Sultan, J. Reeve, and R. Adapa. Combined transient and dynamic analysis of HVDC and FACTS systems. *IEEE Transactions on Power Delivery*, 13(4):1271–1277, 1998.

[10] A. A. van der Meer, R. L. Hendriks, M. Gibescu, and W. L. Kling. Interfacing methods for combined stability and electro-magnetic transient simulations applied to VSC-HVDC. In *Proc. International Conference on Power System Transients*, Delft, the Netherlands, June, 13-17, 2011.